AIChE

Binding Properties of Peptidic Affinity Ligands for Plasmid DNA Capture and Detection

Ying Han
Bio Engineering Lab, Dept. of Chemical Engineering, Monash University, Clayton, Melbourne, VIC 3800, Australia

Sally Gras
The Bio21 Molecular Science and Biotechnology Institute, Dept. of Chemical and Biomolecular Engineering, The University of Melbourne, VIC 3010, Australia

Gareth M. Forde
Bio Engineering Lab, Dept. of Chemical Engineering, Monash University, Clayton, Melbourne, VIC 3800, Australia

DOI 10.1002/aic.11690
Published online December 30, 2008 in Wiley InterScience (www.interscience.wiley.com).

Peptides constructed from α-helical subunits of the Lac repressor protein (LacI) were designed then tailored to achieve particular binding kinetics and dissociation constants for plasmid DNA purification and detection. Surface plasmon resonance was employed for quantification and characterization of the binding of double stranded Escherichia coli plasmid DNA (pUC19) via the lac operon (lacO) to "biomimics" of the DNA binding domain of LacI. Equilibrium dissociation constants (K_D), association (k_a), and dissociation rates (k_d) for the interaction between a suite of peptide sequences and pUC19 were determined. K_D values measured for the binding of pUC19 to the 47mer, 27mer, 16mer, and 14mer peptides were 8.8 ± 1.3 × 10^{-10} M, 7.2 ± 0.6 × 10^{-10} M, 4.5 ± 0.5 × 10^{-8} M, and 6.2 ± 0.9 × 10^{-6} M, respectively. These findings show that affinity peptides, composed of subunits from a naturally occurring operon–repressor interaction, can be designed to achieve binding characteristics suitable for affinity chromatography and biosensor devices. © 2008 American Institute of Chemical Engineers *AIChE J,* 55: 505–515, 2009

Keywords: binding kinetics, peptide ligand design, protein–nucleic acid interactions, surface plasmon resonance, synthetic peptide

Introduction

The need for highly purified plasmid DNA (pDNA) has increased based on the safety and utility of pDNA molecules for vaccine and gene therapy applications.[1–9] In addition, the evolution of biosensors requires that they are increasingly durable and selective, work over large concentration ranges, and are resistant to biofouling,[10] all characteristics which synthetic peptide affinity ligands are able to provide.

In this study, the naturally occurring binding between the *lac* operon DNA domain (*lac*O) and the Lac repressor protein (LacI)[11,12] has been harnessed. The plasmid pUC19 from *Escherichia coli* is chosen as a sample of pDNA for experiments. Plasmid pUC19 is 2686 bp in size and contains two *lac*O-binding domains: *lac*O_1 from bases 180 to 196 and *lac*O_3 from bases 88 to 104. Repression increases significantly with decreasing inter-operator DNA length, indicating that the local Lac repressor concentration at *lac*O_1 is crucial for tight repression.[13] Maximum repression, attributed to sta-

Correspondence concerning this article should be addressed to Y. Han at ying.han@eng.monash.edu.au.

© 2008 American Institute of Chemical Engineers

ble DNA loop formation, was obtained at an operator spacing of 70.5 bp, if the operons are considered to be 20 bp in size. The *lac*O_1 and *lac*O_3 of the pUC19 plasmid are located such as to obtain maximum repression.

The central 17 base pairs of the natural *lac*O_1 sequence have the following sequence (centre of symmetry is in bold):

lacO_1	1	2	3	4	5	6	7	8	9	10	11	12	13	14	15	16	17
	T	T	G	T	G	A	G	C	**G**	G	A	T	A	A	C	A	A

The central 17 base pairs of the natural *lac*O_3 sequence are as follows (center of symmetry is in bold):

lacO_3	1	2	3	4	5	6	7	8	9	10	11	12	13	14	15	16	17
	C	A	G	T	G	A	G	C	**G**	C	A	A	C	G	C	A	A

LacI is a DNA binding protein that regulates expression of the *lac*O. LacI has been studied extensively at the genetic and structural level.[14–20] The DNA binding domain consists of helix I (residues 6–12), a turn, helix II (17–25), helix III (32–45), and the hinge helix IV (50–58),[21] of which helices I and II form a compact helix-turn-helix (HTH) motif whereas helix III packs against the HTH element to complete the hydrophobic core. The repressor's hydrophobic core is formed by hydrophobic residues from all helices I–III with most hydrophilic residues being found at the surface of the molecule. The conventional designation of the HTH is a 20-residue segment, however for the LacI system the helix III completes the hydrophobic core, contributing to the strong LacI/*lac*O affinity interaction. Helix II, often called the recognition helix, is located in the major groove of DNA and rightly deserves this name as at least two side-chain residues are hydrogen bonded directly with DNA bases, two different residues display hydrophobic interactions with DNA, and two residues are shown to be pivotal for DNA binding as substitution almost invariably leads to an I^- mutant.[22]

The in vivo dissociation constant of the Lac repressor and the complete *lac* operator (*lac*O_1, *lac*O_2, and *lac*O_3) has been calculated as 1×10^{-13} M.[23] The in vivo dissociation constant of the Lac repressor and *lac*O_1 alone has been estimated as 5×10^{-10} to 1×10^{-9} M[13] and 1–1.2 $\times 10^{-10}$ M in the presence of a saline buffer and 2.9–3.9 $\times 10^{-11}$ M in the presence of the same saline buffer but with 5% ethylene glycol.[24] In a previous study, a 186 bp double stranded DNA fragment created from a pUC19 template and a 64mer peptide ligand containing the complete LacI DNA binding domain (helix I–helix IV) displayed a dissociation constant (K_D) of 5.7 $\times 10^{-11}$ M.[25,26] As the optimal dissociation constant for an affinity binding mechanism for use in a chromatographic system is 10^{-6} M–10^{-8} M (Natural Toxins Research Centre, 2001), all of these systems display a K_D too low for a chromatographic or adsorption/desorption system such as would be employed in a biosensor. If the dissociation constant is greater than this value, nontarget molecules can be co-purified as the mechanism is normally not strong or selective enough for the target. If the K_D is lower than 10^{-8} M, production yields are low and subsequent cleaning is difficult as the target cannot be eluted from the ligand. Ideally, the binding should be strong enough to avoid leakage during the pDNA application and wash phases, whereas the pDNA should be completely released during the elution phase. The kinetics of the binding and desorption reactions between pDNA and ligands should be suitable for a chromatographic or biosensor system to allow "normal" process flow rates while maintaining specificity.

The problem of finding a suitable ligand in affinity chromatography is not restricted to specificity, but concerns also the binding strength and the kinetics of the ligand-pDNA reaction. This implies that a ligand with an optimized dissociation constant will facilitate the successful operation of affinity chromatography for purification of pDNA. The principal factors on which a comparison of affinity ligands can be based are selectivity, binding capacity, chemical and biological stability, and economics.[27] The specificity of smart ligands is one of the most important factors to be considered in the purification of pDNA. The optimized purification of the Lac repressor by displacement chromatography by Kumar et al. showed that it retained biological activity after immobilization.[28] Hasche and Voβ found that interaction between repressor molecules and RNA was not detectable when interaction with double stranded DNA in the form of a short operator sequence and pDNA occurred.[29,30] Previous affinity approaches have also involved a sequence-specific zinc finger protein and triplex DNA formation, and are not cost-effective. In addition, the triple helix interaction is a commonly used binding method,[31] but has a slow binding kinetics. The feasibility of the affinity approach for pDNA purification using native protein–DNA interaction was positive, but the yield is low owing to the too strong affinity between 64mer peptide and pDNA.[25,26] LacI has also been used in a variety of practical applications.[30,32,33]

One of LacI applications is for affinity purification of pDNA. Affinity purification using DNA binding peptides would offer reduced processing time, less unit operations, and high purity. The current process of pDNA purification usually requires concentration, filtration, and chromatography.[5,34] After the first two processes, dry mass of pDNA is not more than 3% of cell lysate.[35] As a result, a further efficient purification process is essential to quickly capture, concentrate, and purify the pDNA. Affinity chromatography has the purification power to eliminate steps, increase yields and downsize capital equipment, and thereby improve process economics.[36]

Surface Plasmon Resonance (SPR) was employed to analyze biomolecular interactions as it has been proven to be a powerful screening technology for this purpose.[2,37–39] This technique offers significant advantages such as small amounts of analyte sample, being label-free, high sensitivity, and real-time data output for characterizing biomolecular interactions.

Peptides used in this study (see Figure 1) were acetylated after each amino acid addition during peptide synthesis to ensure only full length peptides contained cysteine at their N-terminus. Therefore, immobilization of peptides to chip surfaces was orientation-controlled by conjugation via the thiol group present in the cysteine. In this way, the effect of the presence or absence of the different helical regions on binding characteristics was studied. The SPR biosensor technique was applied to quantify the kinetics of binding between LacI-based peptides (acting as affinity ligands) and double stranded DNA in the form of the plasmid pUC19. The pUC19 contains an optimized *lac* binding region which theoretically can be inserted into any pDNA as an "affinity cas-

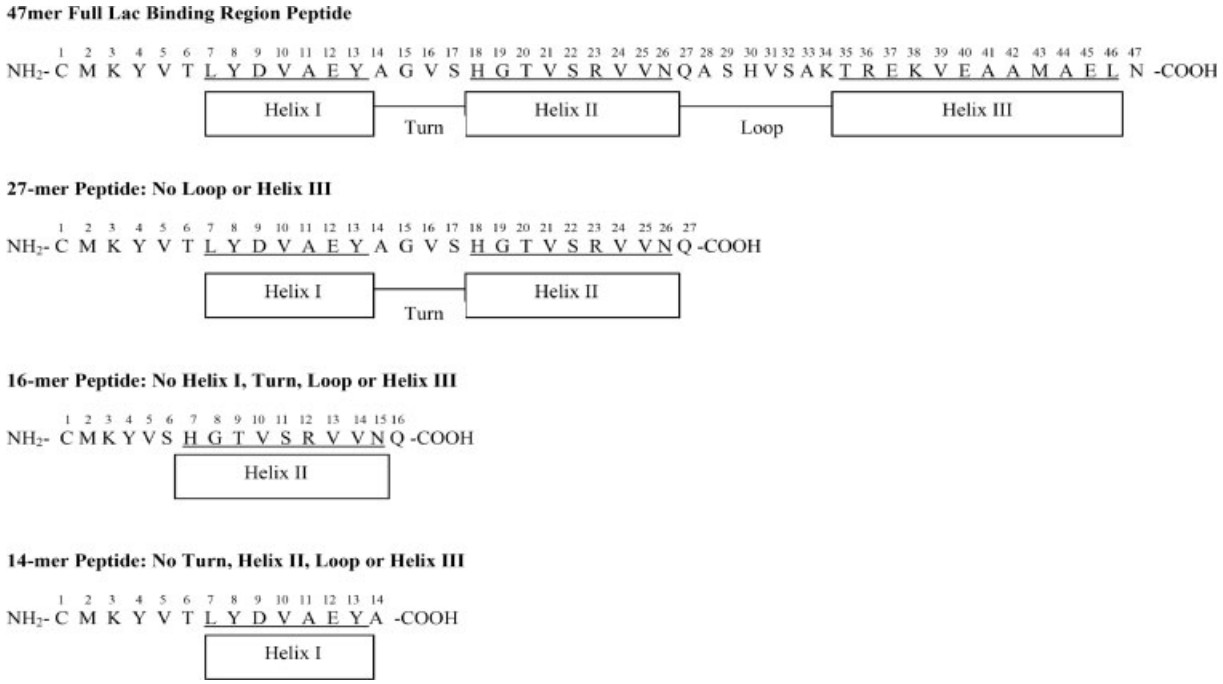

Figure 1. Structures of the tailored biomimetic affinity ligands.

The length and sequence of the 47mer, 27mer, 16mer and 14mer peptides. Synthesis included acetylation after each amino acid to ensure only full length contains cysteine at N-terminus.

sette" to facilitate affinity purifications. We describe the development of an affinity-selective variant of the plasmid binding peptide library approach that utilizes a novel plasmid-binding peptide for purification of the pDNA.

Materials

1 kbp DNA ladder (BioLabs, New England). Agarose and PureYield™ and Wizard® Maxiprep DNA Purification System were purchased from Promega (Madison, WI). Boric acid and sodium formate (M_w 68.01, 98.0%) were from Ajax, Australia. *E. coli*, DH5α (EndA$^-$), and pUC19 plasmid (0.01 μg/l) were purchased from Invitrogen (Victoria, Australia). Ethidium bromide (Sigma, M_w 394.31, 10 mg/ml), ethylenediaminetetraacetic acid (EDTA, M_w 292.3, Serva, USA), *N*-hydroxysuccinmide (NHS), *N*-ethyl-*N*′-(3- diethlamino propyl) carbodiimide hydrochloride (EDC), PDEA (2-(2-pyridyldithio)-ethaneamine), sensor chip C1 (research grade), and HBS-EP buffer were purchased from Pharmacia Biosensor AB (Uppsala, Sweden). Sodium chloride (M_w 58.44, 99.5%) and Tris (hydroxymethyl) aminomethane (M_w 121.14, 99.8%) were purchased from Amresco (OH). Sodium hydroxide, Tris-HCl (M_w 157.6) and other chemicals were purchased from Sigma-Aldrich (St. Louis, USA) and of analytical grade if not stated otherwise.

pEGFP-N1

To investigate the binding specificity of the *lac* operon (*lac*O) sequence contained in the pDNA and its repressor, the LacI protein, another pDNA that does not contain the *lac*O sequence was used in this research called pEGFP-N1 (Clontech laboratories, CA). This plasmid codes for enhanced green fluorescence proteins. pEGFP-N1 is 4733 kb in size. It was purified from JM109 *E-coli* cells. The molecular weight of pEGFP-N1 was 2.924×10^6 g/mol.

The plasmid pEGFP-N1 was selected to conduct a control experiment with the 16mer peptide. From comparison of the restriction map and multiple cloning sites (MCS) of pEGFP-N1 and pUC19 vectors, all restriction sites are unique (http://www.pkclab.org/PKC/vector/pEFGPN1.pdf). Its backbone provides a pUC origin of replication for propagation in *E. coli*. However, the alignment results from Matcher program (data not shown) confirm that there is no identical sequence of *lac*O_1 and *lac*O_3 in pEGFP-N1 as in pUC19. The similar segment sequence of DNA is not within the important region where helix II lies.

Equipment

BIAcore X (BIAcore, Uppsala, Sweden) equipped with C1 sensor chips was from Pharmacia Biosensor AB, Uppsala, Sweden. The gel electrophoresis system was purchased from Bio-rad laboratories, CA, equipped with Gel Doc™ EQ Gel Documentation System and Quantity One™ gel documentation system (Biorad, Hercules, CA). The Wizard Maxipreps DNA Purification System was from Promega and other equipment included: a spectrophotometer (Shimadzu UV-2450, Japan), a centrifuge (Heraeus, multifuge 3 S-R, Germany), a freezer (Nuaire, ultralow freezer, Japan), and an FTIR spectrometer (Varian, CA).

Methods

Bacterial production of pDNA

Plasmid pUC19 (0.01 μg/l, Invitrogen) was transformed and propagated in *E. coli* DH5α (EndA$^-$, Invitrogen,

Australia). A culture of *E. coli* DH5α was grown in LB medium (10 g tryptone, 5 g yeast extract, 5 g NaCl) containing 100 μg/ml ampicillin (Austrapen, CSL, Australia) and was incubated overnight at 37°C. Unused cells were frozen in a dry ice/ethanol bath for 5 min before returning to the −75°C freezer (Ultralow freezer, Nuaire, Japan).

Isolation of pDNA and analysis

Purified pDNA was used to examine the interaction of the repressor proteins with DNA. It was isolated with Promega Maxiprep DNA purification kits (Promega, USA) with purification protocols for high copy number vectors according to the instruction of the manufacturer. TE buffer (10 mM Tris-HCl, 1 mM EDTA, pH 8.0) was used in DNA ladder dilutions. DNA concentrations were determined using absorption measurements at 260 nm (A260) (Shimadzu, UV 2450, Japan).

Gel electrophoresis

The integrity of pDNA and proportion of isoforms was assessed by ethidium bromide gel electrophoresis using 0.8% agarose gels. A 1 kb DNA ladder (Promega, USA) was used as a marker with fragments of 10,000, 8000, 6000, 5000, 4000, 3000, 2000, 1500, 1000, and 500 bp. Ethidium bromide was used at a concentration of 0.05 μg/ml. Gels were electrophoresized at 66 V for 90 min in TAE (Tris-acetate electrophoresis buffer: 10 mM Tris, 10 mM acetate acid, 1 mM EDTA). The staining with ethidium bromide was accomplished during electrophoretic separation and not afterwards which has certainly an effect on detection of nucleic acids in the gels and the separation characteristics. The supercoiled DNA was analyzed with densitometric scanning methods. All the gels were scanned and analyzed using a Quantity One™ gel documentation system (Bio-Rad laboratories, USA).

Restriction endonuclease digestion of purified pDNA

pDNA (pUC19) was treated with EcoR1. Following digestion, the DNA fragments were separated by gel electrophoresis and analyzed as described earlier.[40]

LacI peptides

The *lac*O binding peptides (see Figure 1) were custom synthesized by Mimotopes Pty (Melbourne, Australia). All peptides were synthesized to include acetylation after each amino acid addition to ensure that only full length peptides with the correct sequence contain a single cysteine residue at the N-terminus hence enabling the orientation of the ligand to the chip surface to be controlled. The 47mer peptide was considered the "lead" compound as it most closely biomimics the full DNA binding region of the LacI protein and is composed of the helix I-turn-helix II-loop-helix III binding region with a cysteine residue added at its N-terminus to facilitate conjugation (5000.6 Da). Subunit 27mer (helix I-turn-helix II), 16mer (helix II), and 14mer (helix I) peptides (see Figure 1) were also examined. DMSO at a concentration of 5% v/v was used to increase the solubility of the small molecule peptides.[41]

SPR facilitated binding studies

Experiments were performed using a BIAcore X (BIAcore, Sweden) equipped with a C1 sensor chip. The SPR technique has been used successfully to study the kinetics of a number of biomolecular interactions including those of receptor–ligand interactions.[42] All binding experiments were carried out at 25°C in Hepes-buffered saline (HBS) as running buffer (0.01 M HEPES pH 7.4, 0.15 M NaCl, 3 mM EDTA, 0.005% Surfactant P20, sterile-filtered and degassed, BIAcore, Sweden). Peptides were covalently attached to the surface of a sensor chip and a solution containing the analyte (DNA) was passed over the surface. The binding of molecules to the target attached to the sensor surface generates an evanescent response, which is proportional to the mass of adsorbed molecules.

Immobilization of peptides to C1 sensor chips via the thiol group was performed using 90 μl of PDEA in borate buffer (pH 8.3) on the carboxymethalyted matrix activated with 50 μl of a mixture of 0.2 M EDC and 0.05 M NHS at a ratio of 1:1. Then, 90 μl of peptides (200 μg/ml in formate buffer, pH 4.3) were injected. Finally, 50 μl of 50 mM cysteine in a 1.0 M NaCl solution was used to block the unoccupied sites on the chip. The relatively low level of immobilized target reduces the effect of mass transport from the bulk analyte solution, thereby facilitating kinetic analysis. The C1 chip flow cell No. 1 was left unmodified to act as a control reference cell to minimize variations caused by nonspecific binding and bulk refractive index changes.

pDNA binding was conducted at a flow rate of 30 μl/min to avoid diffusion-controlled kinetics.[43] Serial dilutions of the pDNA were prepared using HBS buffer then loaded onto the BIAcore C1 chip. Plotting the response (RU) against time (seconds) during the course of an interaction provided a quantitative measure of the progress of the interaction. The sensor chip surface was regenerated after each experiment by several injections of 30 μl of 1.0 M NaCl (pH = 11). Checking regeneration was done by repeating analyte and regeneration solution injections while monitoring if the response stays comparable.

Plasmid pUC19 as analyte in the fluid phase was passed over a sensor chip surface immobilized with 16mer peptide. To find suitable buffer conditions for binding, preliminary experiments with one concentration of pDNA (600 μg/ml) in buffers of different ionic strength were carried out. First a basic buffer of 10 mM phosphate buffer was made with 100–750 mM NaCl and binding was monitored. Because of the low flow rate of 10 μl/min, the high amount of immobilized ligand and only one concentration of pDNA, the binding curves obtained were not suitable for determining binding parameters. However, the experiment showed that SPR was a suitable method to investigate *lac*O-LacI binding and that it was possible to monitor the binding event in real time.

It was observed that dissociation curves did not reach the baseline. Depending on contact time and analyte concentration up to 5% of peptides did not decay. Even after prolonged dissociation periods (dissociation time = 2 × association time), a small amount material remained stably bound on the chip and had to be removed by the application of regeneration buffer (pH 11.0, 1 M NaCl).

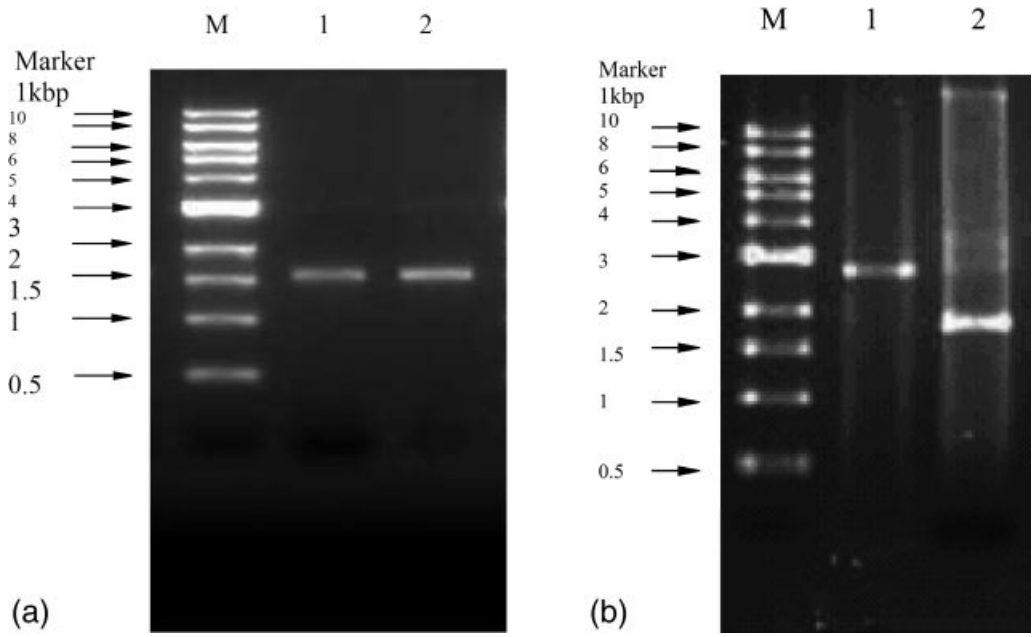

Figure 2. Purified plasmid DNA.

(a) Ethidium bromide agarose electrophoresis gel of purified pDNA which was used in the BIAcore studies. Lane M: 25 μg/ml 1 kbp DNA molecular size marker (10 μl), Lanes 1 and 2: 30 μg/ml pDNA used in studies (diluted $\times$100 from 3000 μg/ml), purified pUC19 sample (10 μl and 20 μl, respectively). The clear apparent band is supercoiled (SC) pDNA. (b) Restriction endonuclease digestion of purified pDNA. Lane M: 25 μg/ml 1 kbp DNA molecular size marker (10 μl), Lane 1: 300 ng pUC19 pDNA sample digested with EcoRI which cuts supercoiled pDNA into linear pDNA (ca. 2.6 kbp). Lane 2: 500 ng pUC19 pDNA sample with no enzymatic digestion.

Nonspecific binding studies

Nonspecific binding studies were carried out by passing pDNA at the requisite dilution over a blank C1 chip surface. The pDNA was serial diluted with HBS buffer (10 mM, pH 7.4). The binding response following each injection was used to determine the degree of nonspecific binding of pDNA to the blank chip surface and/or immobilized peptide surface.

Kinetics data analysis

All kinetic data was studied by direct kinetic analysis and steady-state affinity using BIAevaluation software (version 4.1, Pharmacia Biosensor AB). Experimental curves (i.e., sensorgrams) corresponding to pDNA binding at different concentrations were simultaneously processed. The numerical integration algorithms used by BIAevaluation software are sensitive to the parameters that are set, and may deviate from the true kinetics course if the parameters are not set correctly. Direct and global curve fitting with numerical integration algorithms is an optimum approach for data analysis.[37,44–47] A simple 1:1 (Langmuir) model was applied to fit the data using the numerical integration method. In most cases, rate constants were calculated by global fitting of the association and dissociation phases of the response curves. For experimentally determined parameters, the quoted errors are the standard error reported by BIAevaluation.

Transmission infrared studies

FTIR spectra of 16mer peptide (30 mg/ml) in deuterium oxide (D_2O) (Cambridge Isotope Lab, USA) was recorded after sample preparation at room temperature in a transmission cell fitted with CaF_2 windows and a 5 μm Teflon spacer, continuously purged with dry nitrogen to eliminate water vapor interference. One hundred twenty-eight scans were signal-averaged at a resolution of 2 cm^{-1}. Before FTIR measurements, the 16mer peptide was lyophilized. The background for the cell collected with no sample was automatically subtracted from the data collected for the peptide, and then the subtracted spectra were analyzed using GRAMS/32 software with Lorentzian to deconvolve.

Results and Discussion

Gel electrophoresis analysis of pUC19

As shown in Figure 2a, a single band is present in lanes 1 and 2 which indicate that the pUC19 samples were highly purified. This band was supercoiled (SC) plasmid pUC19 as confirmed by restriction endonuclease digestion of the purified pDNA (Figure 2b).

Nonspecific binding between pDNA and the sensor chip

The aim of this analysis was to be able to eliminate the effect of the bulk refractive index and the nonspecific adsorption of pDNA to the sensor chip surface. The sensorgrams for this study were found to be "square-waved" in shape because of a refractive index jump, confirming that minimal pDNA is bound to the blank surface and that the pDNA dissociates rapidly from the blank chip surface. The kinetic data calculated from the sensorgrams (Table 1, $K_D \approx 10^{-4}$ M) also indicates that the binding between pDNA and the chip exhibits a limited strength of binding. The binding between pDNA to the chip is considered to be predominantly a noncovalent, electrostatic interaction as the pI for pDNA is

Table 1. Comparison of Nonspecific Binding of pUC19 and Binding of pEGFP-N1 to BIAcore Sensor Chip C1 in PBS

pDNA	Association Rate Constant (M^{-1} s^{-1})	Dissociation Rate Constant (s^{-1})	Dissociation Constant (K_D) (M)
pUC19	541 ± 5.3	0.1 ± 0.05	$(2.4 \pm 0.3) \times 10^{-4}$
pEGFP-N1	467 ± 4.6	0.2 ± 0.02	$(4.4 \pm 1.1) \times 10^{-4}$

Data is the mean of two runs ($n = 2$).
± indicates one standard deviation from the mean

approximately 2.1 (data not shown) and the pK_a for the sensor chip surface is 3.5. This is confirmed by an increasing K_D value for increasing salt concentrations in the binding buffer (data not shown). For example, at 150 mM NaCl concentration the binding between the pDNA and chip surface is negligible. The binding of pEGFP-N1 to sensor chip was slightly stronger than the binding of pUC19 because of the stronger negative charge of pUC19 (Table 1). However, affinity interaction experiments eliminated the effect of nonspecific adsorption by subtracting the response from the blank flow cell (flow cell 1) from the peptide conjugated cell (flow cell 2).

Binding between 16mer peptide and pEGFP-N1 as a control experiment to check the binding specificity between 16mer peptide and pUC19

The pEGFP-N1 sequence was confirmed to be another suitable pDNA for use in control experiments to check the selectivity of the binding between pUC19 and the 16mer peptide because there was no binding between 16mer peptide and F3 pEGFP-N1 in HBS buffer (data not shown). Figures 3a,b show the representative subtracted sensorgrams which were obtained after one injection of 600 μg/ml pEGFP-N1 over the chip C1 immobilized with 16mer peptide and blank chip C1. There was a significant difference observed using the biosensor.

Response units of the 16mer peptide to pUC19 were more than double of those of the 16mer peptide to pEGFP-N1 both using HBS buffer and PBS buffer (Table 2). The significant increase in response units suggested that there is strong binding between the 16mer peptide and pUC19 but no same binding with pEGFP-N1. This indicates a strong binding between the 16mer peptide and pUC19, which is attributed to the 16mer peptide specifically binding to lacO contained in pUC19.

Binding of pUC19 to 47mer and 27mer synthetic affinity ligands

Association rates, dissociation rates, and dissociation constants were determined from the sensorgrams, an example of

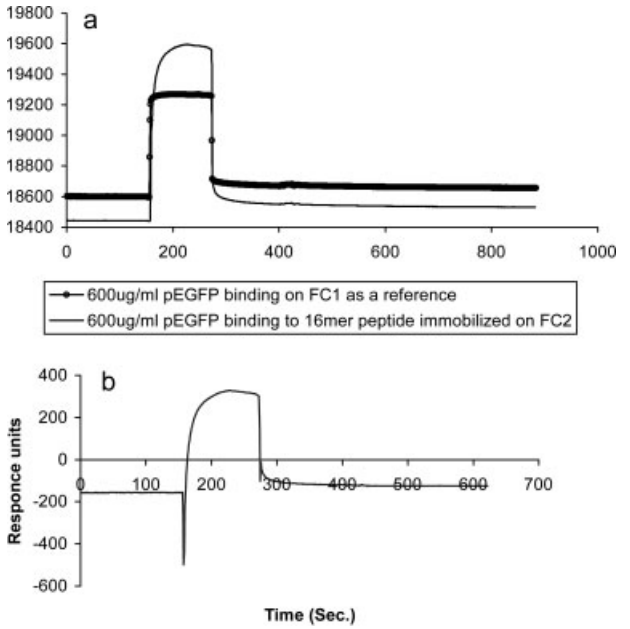

Figure 3. A representative subtracted sensorgram obtained using sensorgram on FC2 subtracting FC1 with BIAevaluation software (version 4.1).

A significant difference in response units was observed when 600 μg/ml of pDNA was injected over the BIAcore sensor chip C1 surface to which the 16mer peptide had been immobilized compared to pDNA injection over a blank chip surface. (a) Two overlayed representative sensorgrams depicting injections of 600 μg/ml pEGFP-N1 over the surfaces with and without the immobilized 16mer peptide. (b) Sensorgram obtained for 600 μg/ml of pEGFP on a BIAcore sensor chip C1 after data for the blank chip presented in (a) above is subtracted from the data for the chip to which the 16mer peptide has been immobilized.

which is shown in Figure 4 for pUC19 binding to the 47mer. The results for each of the ligands are presented in Table 3. The relative magnitudes of the dissociation constants are plotted in Figure 4. As can be seen from this data, all ligands displayed unique rates of association, rates of dissociation, and dissociation constants.

The fastest association rate was for the 27mer followed by the 47mer, the 16mer then the 14mer. The slowest dissociation rate was for the 47mer followed by the 27mer, the 16mer then the 14mer (Figure 5).

Within the limits of experimental error, the dissociation constant (K_D) for the 27mer and 47mer were found to be very similar ($7.2 \pm 0.6 \times 10^{-10}$ M and $8.8 \pm 2.3 \times 10^{-10}$ M, respectively). These dissociation constants were in rea-

Table 2. Binding Response of 16mer Peptide to pEGFP-N1 and pUC19 in PBS and HBS Buffers as Running Buffers

Concentration of 16mer Peptide (μg/ml)	Binding Response in PBS Buffer		Binding Response in HBS Buffer	
	ΔRU_{pEGFP}	ΔRU_{pUC19}	ΔRU_{pEGFP}	ΔRU_{pUC19}
600	32 ± 2	69 ± 5	0	65 ± 5
300	10	55 ± 5	0	50 ± 4
160	0	39 ± 3	0	35 ± 3
10	0	15 ± 1	0	12 ± 1

Sixty microliters of pDNA (pUC19 or pEGFP-N1) was injected over the sensor chip to which the 16mer peptide had been immobilized as a ligand and the response monitored with a BIAcore system. Data is the mean of two runs (n = 2). ± indicates one standard deviation from the mean.

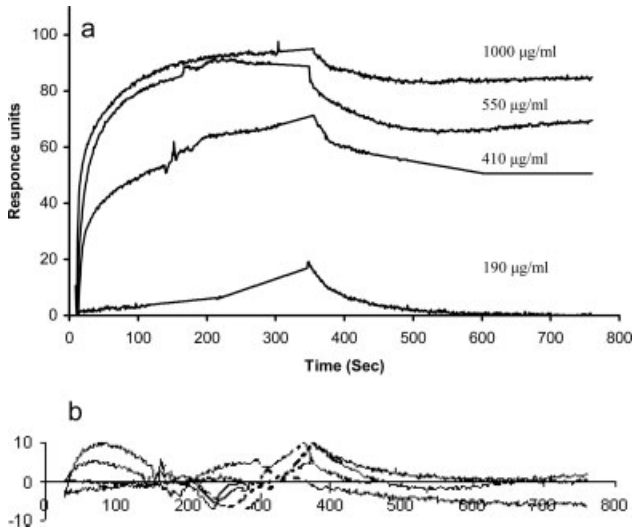

Figure 4. An overlay plot for a typical binding curves obtained from the SPR binding studies.

pUC19 pDNA was injected at various concentrations (10–1000 μg/ml) over the BIAcore chip to which the 16mer peptide was immobilized. From the top curve to bottom curve, the pUC19 pDNA concentrations were 1000, 550, 410, and 190 μg/ml in HEPES-buffered saline. Binding curves were overlaid using BIAevaluation software (version 4.1). The dispersion spikes around the 350 s timepoint indicate the start of the dissociation phase. Figure 4b depicts the residuals while fitting the sensorgrams. The background corrected sensorgrams were fitted to a Langmuir binding model and subsequently used to obtain the k_a, k_d, and K_D values presented in Table 3.

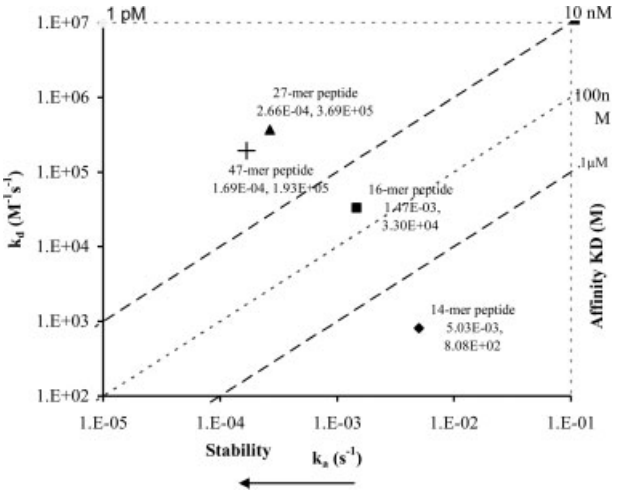

Figure 5. Comparison of association rate and dissociation rate constants and affinity of pUC19 pDNA to LacI-based peptides.

sonable agreement with literature data in that the measured binding was weaker than that of the Lac repressor binding to native DNA (*lac*O_1, *lac*O_2, and *lac*O_3) calculated as 1×10^{-13} M[48] and similar to the *in vivo* dissociation constant of the Lac repressor and *lac*O_1 alone estimated as 5×10^{-10} to 1×10^{-9} M[13] and 1–1.2 $\times 10^{-10}$ M in the presence of a saline buffer and 2.9–3.9 $\times 10^{-11}$ M in the presence of the same saline buffer but with 5% ethylene glycol.[24] More significantly, the dissociation constant was weaker than for a dsDNA fragment containing the pUC19 *lac* binding region (186 bp) interacting with a 64mer peptide which contained helices 1–4 (see Introduction) of 5.7 $\pm$ 0.3 $\times 10^{-11}$ M[25]. Hence, it may be concluded that although the absence of helix III (residues 32–45) has a negligible effect on the overall dissociation constant, its absence appears to increase both the association and dissociation rates. This may be attributed to the presence of helix III sterically hindering the binding of pUC19 to the affinity peptide during the adsorption phase, but once the binding occurs, the presence of the helix III creates a more hydrophobic core further stabilizing the affinity interaction thereby contributing to a decreased dissociation rate.

Most importantly, the dissociation constants of the 27mer and 47mer remained too high ($<10^{-8}$ M) to be considered for use in an affinity chromatography application.

Binding of pUC19 to 16mer and 14mer single helix synthetic affinity ligands

The presence of a single helix (16mer and 14mer) was found to have a much more profound effect on the binding characteristics: the association rates (k_a) were slower, the dissociation rates (k_d) were faster, and the overall affinity interactions were weaker (higher K_D). The slowest association rate and fastest dissociation rate were measured for the 14mer (helix I only) resulting in the weakest affinity interaction (6.2 $\pm$ 0.9 $\times 10^{-6}$ M) that may be considered slightly high ($>10^{-6}$ M) for use in an industrial affinity chromatography application. Of the ligands assessed in this body of work, only the 16mer (helix 2) displayed a dissociation con-

Table 3. SPR Binding Studies Between lacI-based Peptides and Plasmid DNA (pUC19) Which Contains a lacO Binding Region

	Equilibrium			
	Direct Kinetic Analysis			Steady-State Analysis
Peptides	Association Rate Constant (M^{-1} s^{-1})	Dissociation Rate Constant (s^{-1})	Dissociation Constant (K_D)* (M)	Equilibrium Dissociation Constant(M)
Blank	$k_a = 543 \pm 37$	$k_d = 0.1 \pm 0.02$	$K_D = (2.4 \pm 0.5) \times 10-^4$	$K_D = (5.3 \pm 0.5) \times 10^{-5}$
47mer peptide	$k_a = (1.9 \pm 0.8) \times 10^5$	$k_d = (1.7 \pm 0.3) \times 10^{-4}$	$K_D = (8.8 \pm 1.3) \times 10^{-10}$	$K_D = (5.3 \pm 0.9) \times 10^{-8}$
27mer peptide	$k_a = (3.7 \pm 0.5) \times 10^5$	$k_d = (2.7 \pm 0.6) \times 10^{-4}$	$K_D = (7.2 \pm 0.6) \times 10^{-10}$	$K_D = (4.4 \pm 0.8) \times 10^{-9}$
16mer peptide	$k_a = (3.3 \pm 0.1) \times 10^4$	$k_d = (1.5 \pm 0.7) \times 10^{-3}$	$K_D = (4.5 \pm 0.5) \times 10^{-8}$	$K_D = (9.8 \pm 0.8) \times 10^{-8}$
14mer peptide	$k_a = 808 \pm 69$	$k_d = (5.0 \pm 0.9) \times 10^{-3}$	$K_D = (6.2 \pm 0.9) \times 10^{-6}$	$K_D = (9.5 \pm 0.5) \times 10^{-4}$

*Mean of two runs ($n = 2$); $\pm$ indicates one standard deviation from the mean.

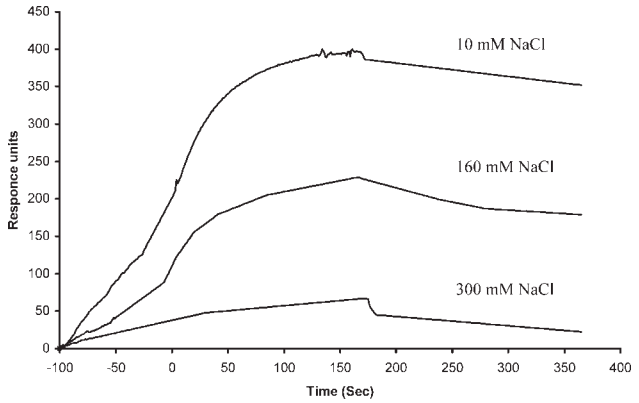

Figure 6. Salt dependence of the binding between pUC19 pDNA and the 16mer peptide.

10, 160, and 300 mM NaCl were added separately into HEPES buffer (0.01 M HEPES pH 7.4, 3 mM EDTA, 0.005% Surfactant P20, degassed and filtered) as running buffers.

stant ($4.45 \pm 0.5 \times 10^{-8}$ M) suitable for employment in an affinity chromatography application.

The 16mer peptide (helix II only) gave rise to a 5.9-fold decrease in k_a compared to the 47mer peptide and an 11.2-fold decrease in k_a compared to the 27mer. In terms of k_d, the 16mer produced an 8.7-fold increase in k_d compared to the 47mer and a 5.5-fold increase compared to the 27mer. This indicates that changes in the association rate contributed the greatest portion of difference to the overall dissociation constant. The same held true for the 14mer in comparison to the 27mer and 47mer. The K_D values were thus increased approximately 56-fold for the 16mer peptide and 7780-fold for the 14mer. From these data, it may be concluded that helix II plays the most critical role of helices I–III in the strength of the affinity interaction.

The dissociation rate and association rate constants as well as dissociation equilibrium constants (10^{-10}–10^{-6} M) of pUC19 plasmid to the designed peptide subunits were significantly lower than those of native *lac*O–LacI interaction (10^{-15}–10^{-10} M).[48] This was in great agreement with the observations on their structure and flexible adaptation in nonspecific and specific protein–DNA interactions. The binding to nonspecific DNA was found faster by several orders of magnitude and speeded up the search for the specific site.[49]

Salt dependence of Lac repressor protein binding to DNA

Figure 6 presents the binding of pUC19 pDNA to the 16mer peptide in response to an increase in NaCl concentration. It was demonstrated that the binding between pUC19 and 16mer peptide is salt dependent as the binding response decreased with increasing NaCl concentration (Figure 6). Maximum binding was observed at 10 mM NaCl, being the lowest salt concentration tested, whereas the lowest binding was observed at 300 mM NaCl. These results imply that binding between pUC19 (analyte) and the 16mer peptide (ligand) are mainly governed by electrostatic forces, although hydrophobic interactions and hydrogen bonding between helix II and the DNA sequence still play an important role.[21,50,51] Indeed, it is likely that subtle changes in electrostatic interactions and hydrogen bonding are responsible for the different DNA binding behavior observed for the 14mer, 16mer, and 27mer ligands and our results highlight how different fragments (helix I, helix II, and helix III) of amino acid sequences from the same repressor protein (14mer, 16mer, 27mer, and 47mer) can dramatically influence DNA binding affinity.

FTIR analysis

For peptide secondary structure, the amide I band (between 1640 and 1660 cm^{-1} of the IR spectrum) was analyzed.[52,53] At this specific region of the FTIR spectrum, the absorption (vibration) of the carbonyl group of the amide bond is analyzed. This group absorbs at typical wavenumbers of the FTIR spectrum, depending on the secondary structure.[52] Secondary structural elements were assigned based on observations previously collated by Goormaghtigh et al (1994).[54]

The amide I band of the FTIR deconvolved spectra of the 16-residue synthetic peptide in D_2O is shown in Figure 7a. D_2O was used as a solvent for analysis rather than H_2O as this allows greater separation between the peaks arising from helix and disordered structure (the peak for disordered structure shifts from near the helix at 1654 cm^{-1} in H_2O to 1645 cm^{-1} in D_2O) and avoids the subtraction of a water background.

The deconvolution procedure results in two decomposed bands (Figure 7b) and a set of positions, bandwidths and

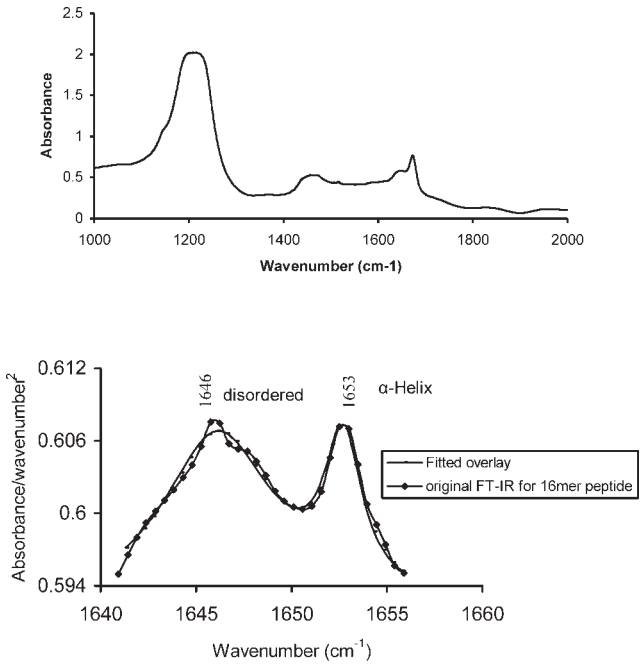

Figure 7. Transmission FTIR absorbance spectrum of 16mer peptide.

FTIR absorbance spectrum (A) and deconvolved spectrum (B) of 16mer peptide in D_2O. The peptide concentration is 30 mg/ml.

Table 4. Band Position and Fractional Band Areas (A*) in D_2O: assignments are based on those presented by Goormaghtigh et al. (1994)

	Band Position in D_2O/cm^{-1}		16mer Peptide in D_2O/cm^{-1} Used in this Study	
Secondary Structure	Average	Extremes	Band Position	Frictional Band Area (*A**) (%)
α-helix	1652	1642–1660	1653	14
β-sheet	1630	1615–1638	0	0
β-sheet	1679	1672–1694	0	0
Disordered	1645	1639–1654	1646	40
Turns	1671	1653–1691	1674	46

*The values of *A* are rounded off to the nearest integer.

areas also shown in Table 4. An absorbance band at 1646 cm^{-1} (associated with disordered structure) can be observed. A second absorbance band in the spectrum for the 16mer peptide is centered at 1653 cm^{-1}. The 1642–1660 cm^{-1} wavenumber range is associated with an α-helical structure, when D_2O is used as a solvent. The 1653 cm^{-1} band of the 16mer peptide indicated that α-helical structure is present in the peptide.

According to the literature,[14–20,49] a combination of electrostatic, hydrophobic, and Hydrogen bonding occurs between the DNA binding sequence and the full LacI protein. For affinity binding between the pDNA and the peptide, it is expected based on data presented in the literature[14–20,49] that binding will be mediated predominantly via electrostatic and Hydrogen bond interactions and that as only one helix of the whole native helix-turn-helix-loop-helix structure is present, that hydrophobic binding will be reduced in comparison to that of the whole protein.

The next step was to confirm that the high-affinity interaction observed between the 16mer ligand and the pUC19 DNA is specific to this DNA sequence and does not occur between the 16mer peptide ligand and other nucleotides that may occur in a cell lysate such as genomic DNA or RNA. The results showed that the pEGFP-N1 pDNA which lacks the *lac* region does not interact with the 16mer ligand. However, previous studies using gel-shift assays indicate that nonspecific interactions can occur between the full length Lac repressor and pET20b(+) DNA which lacks the operator sequence.[29] This nonspecific binding was limited to interactions between the full Lac repressor sequence and double stranded DNA and was not observed for RNA molecules. Hence, our experiments confirm that no binding occurs with molecules other than pDNA containing lac region.

The specificity of the 16mer ligand for pUC19 DNA and other nucleotide sequences will determine whether this ligand can be used as a single purification step for the isolation of pUC19 DNA or an enrichment step, possibly eliminating major contaminants such as proteins, carbohydrates, lipopolysaccharides, and RNA. The ultimate test is to ensure that the 16mer ligand can purify pUC19 DNA from a complex cell lysates feed. This has been shown to be possible in another body of work.[55]

Economic considerations of a peptide affinity approach

As the design of adsorbents that target pDNA (rather than proteins) are improved, the total ligand density required for the commercially viable purification of pDNA will be reduced as more ligand is made available for interaction with pDNA[56–59]. Additionally, because of the volume of global peptide production, peptides have matured to a level where they should effectively be considered a commodity[60,61] rather than being thought of as an extremely expensive biomolecule.

Conclusions

The determination of binding characteristics in naturally occurring systems as they relate to individual segments within larger biological structures, such as those observed here, could be of great value to guide the design and use of affinity ligands for the chromatographic purification of DNA. The peptides were designed as ligands for affinity purification of pDNA, and the importance of helices I–III to the strength of binding was determined using SPR. The method we used provides a quick and cost-effective means to determine whether a peptide has a suitable strength of binding for an affinity mechanism and is hence worthy of further investigation.

The findings indicate that it was possible to design an affinity ligand based on a naturally occurring protein–DNA interaction that has a dissociation constant within the optimal specified range of 10^{-6}–10^{-8} M. Of the ligands assessed, only the 16mer displayed a dissociation constant suitable for employment in a commercial-scale affinity chromatography application for the purification of pUC19. Moreover, the k_d (10^{-3} s^{-1}) of pDNA and 16mer LacI peptide implied that pDNA might dissociate from the chip quickly. This would be desirable for regeneration of the chip and ultimately elution of pDNA in a chromatography system. The *lac* binding region in the pUC19 (optimized *lac*O1 and *lac*O3 region) may act as an "affinity cassette" which may be inserted in any pDNA to facilitate affinity purifications. Helix III showed no or negligible effect on DNA binding but contributed to the complex stability as indicted by a lower dissociation rate. For affinity binding between the pDNA and the peptide, it is expected that based on data presented in the literature[14–20,49] that binding will be mediated predominantly via electrostatic and Hydrogen bond interactions and that as only one helix of the whole, native helix-turn-helix-loop-helix structure is present that hydrophobic binding will be reduced in comparison to that of the whole protein.

The results support the earlier expectation that affinity ligands for pDNA purification can be optimized by a deeper understanding of the contribution made by individual helices to a larger structural motif of binding region. The increasing use of pDNA in gene therapy and vaccine applications requires the production of highly purified pDNA at increasingly larger scales. Current approaches for purifying pDNA from bacterial production systems exploit the physiochemical properties of nucleic acids in nonspecific capture systems. These findings could impact on the viability of affinity methods for the production of commercially viable amounts of

pDNA for DNA vaccine and gene therapy applications. Additionally, the reported method may be harnessed to design nucleic acid affinity sensors for the detection of specific nucleic acid targets in complex biological samples without the need for amplification or labeling.

Acknowledgments

This work was supported by an Innovation Fellowship from the Victorian Endowment for Science, Knowledge and Information (VESKI) and a Monash University Engineering Faculty Research Grant.

Notation

bp = base pairs
HTH = helix-turn-helix motif
k_a = association rate of binding
k_d = dissociation rate of binding
K_D = equilibrium dissociation constant
LacI = Lac repressor protein
pDNA = plasmid DNA
RU = response units
SPR = Surface plasmon resonance

Literature Cited

1. Boniface JJ, Davis MM. The kinetics of binding of peptide/MHC complexes to T-cell receptors: application of surface plasmon resonance to a low -affinity measurement. *Methods: A Companion to Methods in Enzymology*. 1994;6:168–176.
2. Bouchie A. Box 1 FDA, NCI collaborate to identify biomarkers for cancer trials. *Nat Biotechnol*. 2003;21:718.
3. Danquah MK, Forde GM. Rapid therapeutic plasmid DNA isolation: addressing the looming vaccine crisis. BIOFORUM EUROPE, ISSN 1611-597X,10:24–27,2006.
4. Diogo MM, Ribeiro SC, Queiroz JA, Monteiro GA, Tordo N, Perrin P, Prazeres DM. Production, purification and analysis of an experimental DNA vaccine against rabies. *J Gene Med*. 2001;3:577–584.
5. Forde GM. Rapid-response vaccines-does DNA offer a solution? *Nat Biotechnol*. 2005;23:1059–1062.
6. Fukumoto S, Tamaki Y, Okamura M, Bannai H, Yokoyama N, Suzuki T, Igarashi I, Suzuki H, Xuan X. Prime-boost immunization with DNA followed by a recombinant vaccinia virus expressing P50 induced protective immunity against Babesia gibsoni infection in dogs. *Vaccine*. 2007;25:1334–1341.
7. Johansen P, Raynaud C, Yang M. Anti-mycobacterial immunity induced by a single injection of M-leprae Hsp65-encoding plasmid DNA in biodegradable microparticles. *Immunol Lett*. 2003;90:81–85.
8. Michel ML, Davis HL, Schleef M. DNA-mediated immunization to the hepatitis-B surface-antigen in mice-aspects of the humoral response mimic hepatitis-B viral infection in humans. *Proc Natl Acad Sci USA*. 1995;92:5307–5311.
9. Wolff JA, Malone RW, Williams P, Chong W, Acsadi G, Jani A, Felgner PL. Direct gene transfer into mouse muscle in vivo. *Science*. 1990;247:1465–1468.
10. Rogers KR. Recent advances in biosensor techniques for environmental monitoring. *Anal Chim Acta*. 2006;568:222–231.
11. Gilbert W, Müller HB. The lac operator is DNA. *Proc Natl Acad Sci USA*. 1967;58:2415–2421.
12. Sadler JR, Sasmor H, Betz JL. A perfectly symmetric lac operator binds the lac repressor very tightly. *Proc Natl Acad Sci USA*. 1983;80:6785–6789.
13. Oehler S, Eismann ER, Krämer H, Müller-Hill B. The three operators of the lac operon cooperate in repression. *EMBO J*. 1990;9:973–979.
14. Barker A, Fickert R. Operator search by mutant Lac repressors. *J Mol Biol*. 1998;278:549–558.
15. Barkley MD, Bourgeois S. *Repressor Recognition of Operator and Effectors*. NY: Cold spring Harbor Laboratory Press, 1980.
16. Bell CE, Lewis M. The Lac repressor: a second generation of structural and functional studies. *Curr Opin Struct Biol*. 2001;11:19–25.
17. Chakerian AE, Matthew KS. Effect of lac repressor oligomerization on regulatory outcome. *Mol Microbiol*. 1992;6:963–968.
18. Kisters-Woike B, Lehming N. A model of the lac repressor-operator complex based on physical and genetic data. *Eur J Biochem*. 1991;198:411–419.
19. Markiewicz P, Kleina LG. Genetic studies of the lac repressor XIV. Analysis of 4000 altered Escherichia coli lac repressors reveals essential and non-essential residues, as well as "spacers" which do not require a specific sequence. *J Mol Biol*. 1994;240:421–433.
20. Steitz TA. Structural studies of protein–nucleic acid interaction: the sources of sequence-specific binding. *Q Rev Biophys*. 1990;23:205–280.
21. Lewis M, Chang G, Horton NC, Kercher MA, Pace HC, Schumacher MA, Brennan RG, Ponzy L. Crystal structure of the lactose operon repressor and its complex with DNA and inducer. *Science*. 1996; 271:1247–1254.
22. Kleina LG, Miller JH. Genetic studies of the lac repressor. XIII. Extensive amino acid replacements generated by the use of natural and synthetic nonsense suppressors. *J Mol Biol*. 1990;212:295–318.
23. David LN, Michael MC. *Principles of Biochemistry*. New York: W. H. Freeman and Company, 2005.
24. Fried MG, Stickle DF, Smirnakis KV, Adams C, MacDonald D, Lu P. Role of hydration in the binding of lac repressor to DNA. *J Biol Chem*. 2002;277:50676–50682.
25. Forde GM, Ghose S, Slater NKH, Hine AV, Darby AJ, Hitchcock AG. LacO-LacI interaction in affinity adsorption of plasmid DNA. *Biotechnol Bioeng*. 2006;95:67–75.
26. Ghose S, Forde GM, Slater NKH. Affinity adsorption of plasmid DNA. *Biotechnol Prog*. 2004;20:841–850.
27. Clonis YD. Affinity chromatography matures as bioinformatics and combinatorial tools develop. *J Chromatogr A*. 2006;1101:1–24.
28. Kumar A, Galaev IY, Mattiasson B. Purification of *Lac* repressor protein using polymer displacement and immobilization of the protein. *Bioseparation*. 1999;8:307–316.
29. Hasche A, Voβ C. Immobilisation of a repressor protein for binding of plasmid DNA. *J Chromatogr A*. 2005;1080:76–82.
30. Lundeberg J, Wahlberg J, Uhlen M. Affinity purification of specific DNA fragments using a *lac* repressor fusion protein. *Genet Anal Tech Appl*. 1990;7:47–52.
31. Schluep T, Cooney CL. Purification of plasmid DNA by triplex affinity interactions. *Nucl Acids Res*. 1998;26:4524–4528.
32. Darby RAJ, Hine AV. LacI-mediated sequence-specific affinity purification of plasmid DNA for therapeutic applications. *The FASEB J*. 2005;19:801–803.
33. Hu MC, Davidson N. Targeting the *Escherichia coli* lac repressor to the mammalian cell nucleus. *Gene*. 1991;99:141–150.
34. Ferreira GNM, Monteiro GA, Prazeres DMF, Cabral JMS. Downstream processing of plasmid DNA for gene therapy and DNA vaccine applications. *Trends Biotechnol*. 2000;18:380–388.
35. Stadler J, Lemmens R, Nyhammar T. Plasmid DNA purification. *J Gene Med*. 2004;6:54–66.
36. Lowe CR, Lowe AR, Gupta G. New developments in affinity chromatography with potential application in the production of biopharmaceuticals. *J Biochem Biophys Methods*. 2001;49:561–574.
37. Majka J, Speck C. Analysis of protein–DNA interactions using surface plasmon resonance. *Adv Biochem Eng Biotechnol*. 2007;104: 13–36.
38. Pattnaik P. Surface plasmon resonance—applications in understanding receptor–ligand interaction *Appl Biochem Biotechnol*. 2005;126: 79–92.
39. Schubert F, Zettl H, Hafner W. Comparative thermodynamic analysis of DNA–protein interactions using surface plasmon resonance and fluorescence correlation spectroscopy. *Biochemistry*. 2003;42: 10288–10294.
40. Tweedie JW, Stowell KM. Quantification of DNA by agarose gel electrophoresis and analysis of the topoisomers of plasmid and M13 DNA following treatment with a restriction endonuclease or DNA topoisomerase I. *Biochem Mol Biol Educ*. 2005;33:28–33.
41. Ciolkowski ML, Fang MM, Lund ME. A surface plasmon resonance method for detecting multiple modes of DNA-ligand interactions. *J Pharm Biomed Anal*. 2000;22:1037–1045.

42. Rich RL, Myska DG. Advances in surface plasmon resonance biosensor analysis. *Curr Opin Biotechnol*. 2000;11:54–61.
43. Adamczyk M, Moore JA, Yu Z. Application of surface plasmon resonance toward studies of low molecular weight antigen–antibody binding interactions. *Methods*. 2000;20:319–328.
44. Karlsson R, Falt A. Experimental design for kinetic analysis of protein-protein interaction with surface plasmid resonance biosensors. *J Immunol Methods*. 1997;200:121–133.
45. Katsamba PS, Park S, Laird-Offringa IA. Kinetics studies of RNA–protein interactions using surface plasmon resonance. *Methods*. 2002;26:95–104.
46. Pabbisetty KB, Yue X. Kinetic analysis of the binding of monomeric and dimeric ephrins to Eph receptors: Correlation to function in a growth cone collapse assay. *Protein Sci*. 2007;16:355–361.
47. Wilkinson CRM, Seeger M, Hartmann-Petersen R, Stone M, Wallace M, Semple C, Gordon C. Proteins containing the UBA domain are able to bind to multi-ubiquitin chains. *Nat Cell Biol*. 2001;3: 939–943.
48. Winter RB, von Hippel PH. Diffusion-driven mechanism of protein translocation on nucleic acids. II. The *E. coil* repressor–operator interaction: equilibrium measurements. *Biochemistry*. 1981;20: 6948–6960.
49. Kalodimos CG, Biris N, Bonvin AM, Levandoski MM, Guennuegues M, Boelens R, Kaptein R. Structure and flexibility adaptation in nonspecific and specific protein–DNA complexs. *Science*. 2004;305:386–389.
50. Lauria A, Montalbano A, Barraja P, Dattolo G, Almerico AM. DNA minor groove binders: an overview on molecular modeling and QSAR approaches *Curr Med Chem*. 2007;14:2136–2160.
51. Normanno D, Vanzi F, Pavone FS. Single-molecule manipulation reveals supercoiling-dependent modulation of lac repressor-mediated DNA looping. *Nucl Acids Res*. 2008;36:2505–2513.
52. Arrondo JLR, Muga A, Castresana J, Goni FM. Quantitative studies of the structure of proteins in solution by Fourier-transform infrared spectroscopy. *Prog Biophys Mol Biol*. 1993;59:23–56.
53. Haris PI, Chapman D. Does Fourier-transform infrared spectroscopy provide useful information on protein structures? *Trends Biochem Sci*. 1992;17:328–333.
54. Goormaghtigh R, Caulaux V, Ruysschart JM. Determination of soluble and membrane protein structure by Fourier transform infrared spectroscopy, III. Secondary structures. *Subcell Biochem*. 1994;23:329–362.
55. Han Y, Forde GM. Single step purification of plasmid DNA using peptide ligand affinity chromatography. *J Chromatogr B*. (available online doi:10.1016/jchromb.2008.08.025).
56. Branovic K, Forcic D, Ivancic J, Strancar A, Barut M, Kosutic Gulija T, Zgorelec R, Mazuran R. Application of short monolithic columns for fast purification of plasmid DNA. *J Chromatogr B*. 2004;801:331–337.
57. Danquah MK, Forde GM. The suitability of DEAE-Cl active groups on customized poly(GMA-*co*-EDMA) continous stationary phase for fast enzyme-free isolation of plasmid DNA. *J Chromatogr B*. 2007;853:38–46.
58. Danquah MK, Ho J, Forde GM. Performance of R-N(R′)-R″ functionalised poly(glycidyl methacrylate-*co*-ethylene glycol dimethacrylate) monolithic sorbent for plasmid DNA adsorption. *J Separation Sci*. 2007;30:2841–2850.
59. Urthaler J, Schlegl R, Podgornik A, Strancar A, Jungbauer A, Necina R. Application of monoliths for plasmid DNA purification: development and transfer to production. *J Chromatogr A*. 2005; 1065:93–106.
60. Ranbaxy. *Jupiter Bioscience Enter into Marketing Tie-Up*. New Delhi, India: The Economic Times.
61. Morreale G, Lee EG, Jones DB, Middelberg APJ. Bioprocess-centered molecular design (BMD) for the efficient production of an interfacially active peptide. *Biotechnol Bioeng*. 2004;87:912–923.

Manuscript received Jan. 10, 2008, and revision received Sept. 4, 2008.